



DETERMINATION BY NUMERICAL MODELING OF STRESS-STRAIN VARIATIONS RESULTING FROM GALLERY CROSS-SECTION CHANGES IN A LONGWALL TOP COAL CAVING PANEL

^{1,*} Mehmet MESUTOĞLU , ¹ İhsan ÖZKAN , ² Alfonso RODRIGUEZ-DONO 

¹ Konya Technical University, Engineering and Natural Sciences Faculty, Mining Engineering Department,
Konya, TÜRKİYE

² Universitat Politècnica de Catalunya (UPC), Civil and Environmental Engineering Department, Barcelona,
SPAIN

¹ mmesutoglu@ktun.edu.tr, ¹ iozkan@ktun.edu.tr, ² alfonso.rodriquez@upc.edu

Highlights

- Significance of sustainability and efficiency in global coal mining.
- Transition to deeper underground mining due to increased coal demand.
- Numerical modeling crucial for understanding and addressing gallery cross-sectional variation.
- Understanding the impact of gallery cross-sectional variation is crucial for safe and efficient mining operations.



DETERMINATION BY NUMERICAL MODELING OF STRESS-STRAIN VARIATIONS RESULTING FROM GALLERY CROSS-SECTION CHANGES IN A LONGWALL TOP COAL CAVING PANEL

^{1,*} Mehmet MESUTOĞLU , ¹ İhsan ÖZKAN , ² Alfonso RODRIGUEZ-DONO 

¹ Konya Technical University, Engineering and Natural Sciences Faculty, Mining Engineering Department,
Konya, TÜRKİYE

² Universitat Politècnica de Catalunya (UPC), Civil and Environmental Engineering Department, Barcelona,
SPAIN

¹ mmesutoglu@ktun.edu.tr, ¹ iozkan@ktun.edu.tr, ² alfonso.rodriguez@upc.edu

(Received: 27.12.2023; Accepted in Revised Form: 07.02.2024)

ABSTRACT: As a major pillar of global energy production, coal mining requires continuous advancements in efficiency to contribute to the broader goal of energy sustainability, all the while the shift towards more sustainable energy sources is underway. Mechanized excavation systems employed in underground coal mines, particularly within the longwall mining method, enable high-tonnage coal production. The Longwall Top Coal Caving (LTCC) method, one of the longwall mining techniques, has been developed for the effective extraction of coal from thick coal seams. However, as mining operations delve deeper, various complex issues, such as gallery cross-sectional variation, emerge. Gallery cross-sectional variation can increase the risk of collapse by affecting the stress distribution in the rock mass, posing a threat to worker safety. This study centers on the numerical modeling and analysis of gallery cross-sectional variation in the Ömerler underground mine, operated by the Turkish Coal Enterprises (TKI), West Lignite Enterprise (GLI). To achieve this objective, an extensive database was established through field and laboratory rock mechanics studies. This database was then utilized in the Fast Lagrangian Analysis of Continua 3D (FLAC3D) (v6.0) program to simulate the cross-sectional variations of the A6 panel in the Ömerler underground mine. The numerical simulation results provide valuable insights into the secondary stress-deformation changes associated with gallery cross-sectional variation.

Keywords: Gallery cross-section, FLAC 3D, Longwall mining, Numerical modeling, Strata control

1. INTRODUCTION

As coal mining remains a crucial component of global energy production, the significance of sustainability and efficiency in this sector is continuously on the rise [1,2]. In 2022, global coal consumption experienced a notable surge of 3.3%, reaching a total of 8.3 billion tons [3]. The ongoing increase in global coal demand has led to a necessity for a shift toward deeper underground mining practices due to diminishing open-pit reserves [4]. This transition imposes a compelling demand on the coal mining industry to improve both sustainability and operational efficiency.

In recent years, the implementation of mechanized excavation systems, particularly in the longwall mining method within underground coal mines, has facilitated high-tonnage coal production [5,6,7]. The Longwall Top Coal Caving (LTCC) method, one of the longwall mining techniques, has been specifically developed for underground coal mining, enabling the effective and efficient extraction of thick coal seams [8,9,10,11,12].

LTCC is considered a safer alternative compared to traditional longwall mining methods [11,13,14]. The controlled collapse process enhances worker safety. However, as mining operations employing the LTCC method delve deeper, they bring forth various complex challenges. One of these challenges is the increasingly significant gallery cross-sectional variation as mining progresses to deeper levels. Gallery cross-sectional variation refers to the alteration of dimensions, shape, or position of the mine gallery as it advances into the depths. It can significantly influence the stress distribution of rock masses and also can

*Corresponding Author: Mehmet MESUTOĞLU, mmesutoglu@ktun.edu.tr

increase the risk of collapse, jeopardizing the safety of mine workers. Additionally, gallery cross-sectional variation has the potential to escalate mining operational costs and negatively impact productivity. Miners seek innovative and secure solutions to overcome this challenge and extract coal reserves as efficiently as possible.

The numerical modeling and analysis of gallery cross-sectional variation can play a crucial role in understanding and addressing these issues. Furthermore, such analyses can serve as a critical tool in finding ways to make mining operations more efficient and safer [15, 16]. Therefore, gallery cross-sectional variation has become an important topic to be addressed in the context of modern coal mining.

An example of the mentioned problem occurred during the implementation of the LTCC method in the Ömerler underground mine, operated by the West Lignite Enterprise (GLI), a subsidiary of Turkish Coal Enterprises (TKI). During coal production and advancement in the production direction within the mine, a situation arises where the transition support units, in the sizing of the gallery, require scanning and widening operations, essentially being unable to pass through the horseshoe gallery sections. As a result, pressures within the face increase during production, often necessitating additional reinforcement. This condition, along with scanning operations, leads to time loss and creates problems for the smooth progress of the waiting coal face.

This paper presents the establishment of a comprehensive database through in-situ and laboratory rock mechanics studies to facilitate the numerical modeling of potential cross-sectional variations in the trackways in the existing conditions of the Ömerler underground mine. Utilizing this extensive database, the FLAC3D (v6.0) program is employed to accurately simulate the secondary stress-deformation alterations that could arise during the transition from a horseshoe cross-section to a trapezoidal cross-section for the A6 panel. The outcomes of these numerical simulations provide valuable insights into the anticipated changes in secondary stress-deformation characteristics.

2. STUDY SITE

TKI-GLI Ömerler Underground coal mine is located in the town of Tunçbilek, (Tavşanlı district of Kütahya province) in Turkey (Fig. 1).

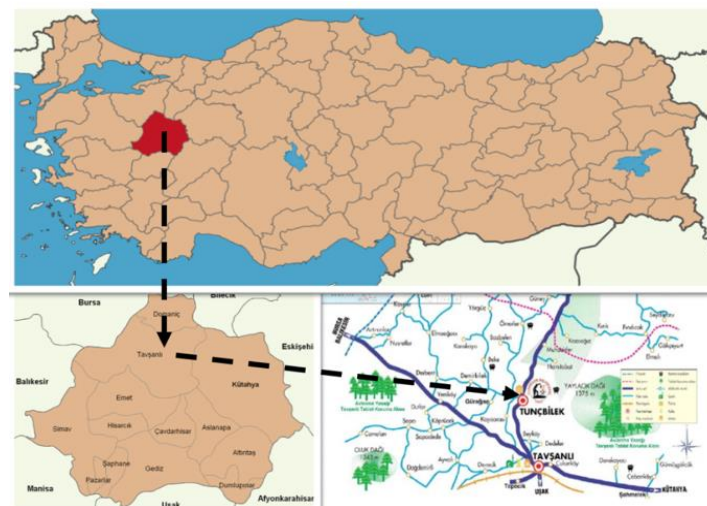


Figure 1. Location of study site

The rock units within the Tunçbilek series are grouped into three main categories, namely Shale, Calcareous Marl, and Marl. The Shale formation, which surrounds the coal seam, is also subdivided into three subgroups. These subgroups consist of the soft shale layer located immediately above the coal seam with a thickness ranging from 20 to 50 cm, the roof shale forming the main roof rock of this formation, and the floor shale formations situated beneath the coal seam (Fig 2).

In the GLI Tunçbilek coal basin, underground coal production has been carried out in the Ömerler-A field. In this underground mine, a fully mechanized mining system is used, and coal extraction is performed using the LTCC method. The thick coal seam, averaging 8 m in thickness, is excavated using a single-pass method for the lower 3.5 m, while the remaining approximately 5 m at the roof level is extracted through the backfilling process, (controlled caving operation), (Fig 2).

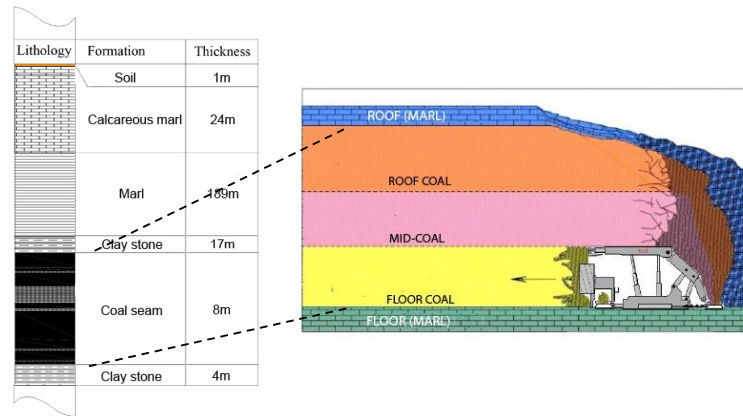


Figure 2. Lithology of geological structure

In the basin, strata have generally dip angles ranging from 5 to 20° toward the northeast. The coal reserve within the study area is estimated to be around 18 million tons. The coal seam thickness varies between 5-12 m, with an average thickness of 8 m [17]. The coal seam contains clay partings of approximately 15-30 cm thickness at various levels. The deepest working section in the underground mine is located at a sea level elevation of +469, and the thickness of the overlying strata is approximately 330 m. The study area is the A6 longwall panel in the Tunçbilek Ömerler underground coal mine (Fig 3) in this research. Rock mass and material property determination studies for coal and surrounding rocks were carried out in the A1, A2, and A6 panels.

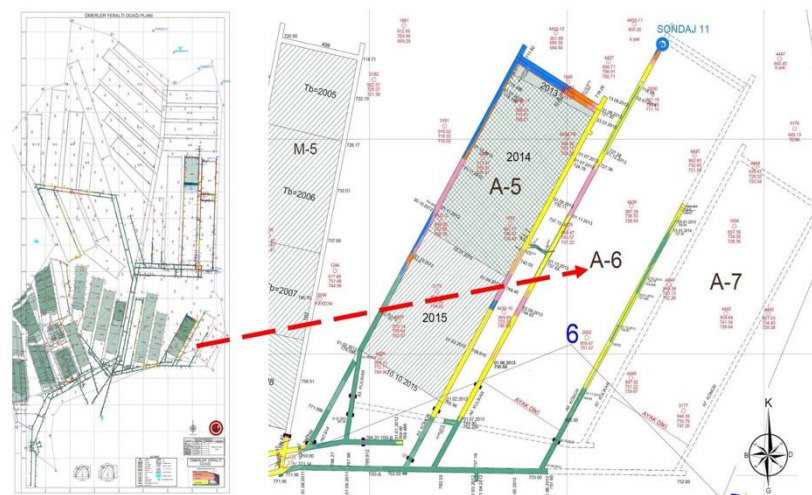


Figure 3. The view of the A6 longwall panel considered in gallery cross-section design studies on the mine layout

3. DETERMINATION OF ROCK MASS AND ROCK MATERIAL PROPERTIES

In the design studies aiming to analyze the cross-sectional variation of the A6 longwall panel galleries

in the Ömerler underground coal mine, on-site and laboratory investigations were conducted to determine rock mass and material properties. These studies encompassed not only the A6 longwall panel where the implementation occurred but also the A1 and A2 longwall panels, where preparatory and production activities are currently in progress.

Underground drilling operations and block extraction studies were carried out in specific underground areas to determine rock mass and material properties, contributing to classification studies. Drilling activities were conducted in the production panel in four directions. Additionally, 50 blocks were extracted from the A1 and A2 panels and transported to the laboratory for sample collection (Fig 4). Moreover, Schmidt hammer rebound hardness tests, point load strength index tests, and plate loading tests were conducted in the A1, A2, and A6 panels.



Figure 4. Typical images from the drilling and block extraction operations conducted in the Ömerler underground mine

All rock mechanics tests were performed on the rock material samples obtained from the blocks transported to the laboratory and the drilling cores. The resulting database is presented in Table 1 [18,19]. Field-based GSI classification studies were conducted in the A1 preparatory gallery for rock mass classifications. The determined values, along with results from other rock mass classification systems, were calculated and presented in Table 2 [18,19].

Table 1. Rock material properties of Ömerler underground mine

| Data | Symbol, Unit | Coal | Roof Rock | Floor Rock |
|---------------------------------------|-------------------------------|-------|-----------|------------|
| Uniaxial compressive strength (UCS) | σ_{ci} (MPa) | 8.84 | 10.66 | 12.04 |
| Tensile strength (Indirect-Brazilian) | σ_t (MPa) | 2.30 | 8.31 | 8.91 |
| Cohesion | c (MPa) | 0.401 | 0.487 | 0.419 |
| Friction angle | φ (°) | 31.03 | 24.32 | 25.44 |
| Modulus of elasticity | E (MPa) | 2663 | 3198 | 3612 |
| Poisson ratio | ν (-) | 0.18 | 0.264 | 0.27 |
| Bulk density | ρ (gr/cm ³) | 1.26 | 2.00 | 2.12 |
| Natural unit weight | γ (kN/m ³) | 12.40 | 19.60 | 21.7 |
| Slake durability index | I_{d2} (%) | 91.00 | 98.89 | 98.55 |
| Point load strength index | $I_{s(50)}$ (MPa) | 0.51 | 0.70 | 2.38 |

The rock mechanics studies revealed that the material and mass properties of the coal unit were weaker compared to the roof and floor units. It was determined that the floor unit exhibited better mechanical properties.

Table 2. Rock mass properties of the Ömerler underground mine

| Data | Symbol, Unit | Coal | Roof Rock | Floor Rock |
|--------------------------------------|---------------------|--------|-----------|------------|
| Geological Strength Index | GSI | 35 | 43 | 47 |
| Rock Mass Rating | RMR | 32 | 44 | 47 |
| Rock Quality Designation | RQD | 50 | 60 | 70 |
| Quantitative Rock Mass Rating | Q | 0.37 | 0.99 | 1.16 |
| Uniaxial compressive strength | σ_{cm} (MPa) | 1.481 | 1.244 | 1.543 |
| Tensile strength | σ_{tm} (MPa) | 0.004 | 0.024 | 0.037 |
| Cohesion | c_m (MPa) | 0.401 | 0.487 | 0.419 |
| Friction angle | φ_m (°) | 31.03 | 24.32 | 25.44 |
| Modulus of elasticity | E_m (MPa) | 302 | 625.99 | 920.07 |
| Poisson ratio | ν | 0.18 | 0.264 | 0.27 |
| Bulk modulus ($K = [E/3(1-2\nu)]$) | K (MPa) | 157.29 | 442.08 | 666.72 |
| Shear modulus ($G = [E/2(1+\nu)]$) | G (MPa) | 127.97 | 247.62 | 362.23 |

To make accurate predictions for the stability of underground openings, the mechanical properties of the rock mass and measurements of the primary stresses in the environment are necessary [20]. In this context, primary stress analysis studies were conducted within the A1 longwall panel of the Ömerler underground coal mine (Fig 5). Following the approach proposed by Aydan [21] for determining the primary in-situ stresses using the fault slip method, the analysis results indicated that the maximum horizontal stress is approximately oriented in the north-south direction. Furthermore, it was determined that at a depth of 300 meters, the largest horizontal primary stress ($P_H = 6.74$ MPa) in the A1 panel is oriented parallel to the gate axis.

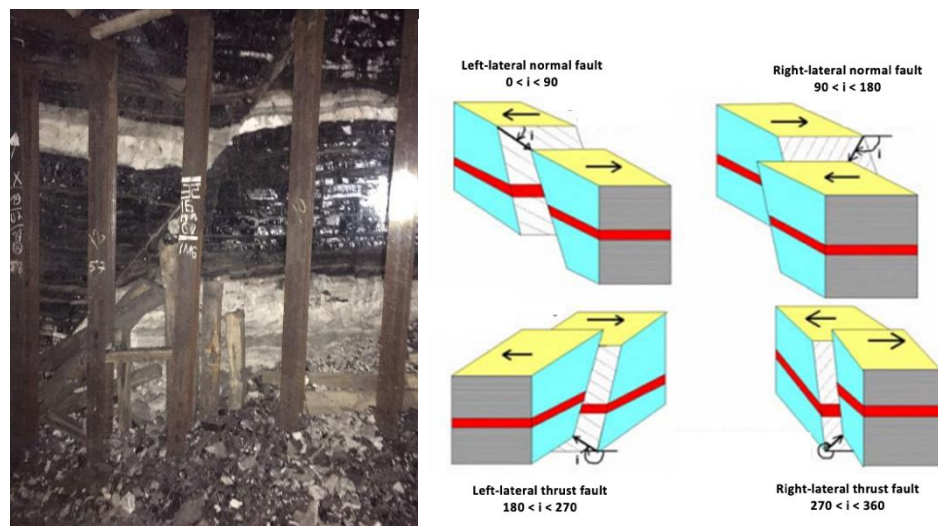


Figure 5. (a) Measurement of primary in-situ stress in a coal seam fault example (b) Definition and measurement of fault lines [21]

3.1. Dimensioning Studies for Gallery Cross-Sectional Change

TKI-GLI operation plans to open new galleries in trapezoidal section in the Ömerler underground mine. The reason for this is that the horseshoe section is not suitable for the comfortable execution of the support units, especially at the foot beginnings in the production panels. The second reason is that the useful cross-sectional area of the horseshoe gallery section is not satisfactory for the operations in the mine. For these reasons, the gallery cross-sectional design studies for the A6 panel of the Ömerler underground coal mine have been modeled in three dimensions for both horseshoe and trapezoidal sections. The stress-

deformation variations occurring in the A6 headgate between the trapezoidal and horseshoe sections have been examined.

Figure 6 presents the existing gallery section of the Ömerler underground coal mine operated by TKI-GLI. According to the dimensions specified here, the width of the gallery is 4600 mm, and the gallery height is 3970 mm. Accordingly, the current gallery section is 18.26 m². However, due to closures occurring in the gallery opening, this gallery section can drop to approximately 13 m² in some areas of the mine.

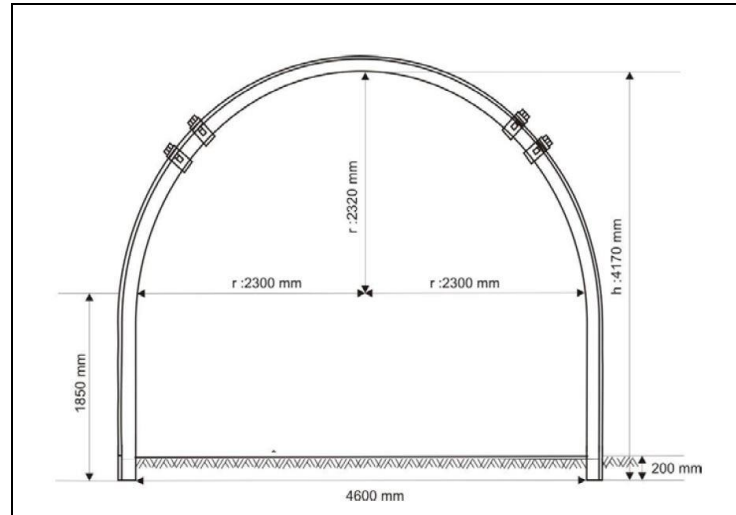


Figure 6. Dimensions of the existing horseshoe gallery section at the Ömerler coal mine

During the dimensioning studies for the trapezoidal gallery section, the opinions of the operation officials were taken, and the situation of the openings in the trapezoidal section opened in some parts of the existing base roads was considered. In addition, the optimum expansion of the useful cross-sectional area has also been a determining factor in the dimensioning of the trapezoidal gallery section to be opened.

In the dimensioning process of the gallery section in underground openings, it is obvious that the mine must be subjected to ventilation in an optimum manner. Therefore, in the dimensioning studies of the gallery section, a ventilation project carried out in the Ömerler underground mine in 2017 was considered. In the ventilation project conducted by Fişne et al. [22], it was stated that the required air velocity for the Ömerler underground mine was 0.5 m/s in the base roads and 1.0 m/s inside the foot. It was also mentioned that the calculated required air volume for the mine is 2591 m³/min, and the 4040 m³/min of clean air entering the mine would be sufficient for the mine. Therefore, it is seen that the newly dimensioned trapezoidal section added to the bottom row of Table 3 is in accordance with the calculated clean air (required) volume for the mine.

Figure 7 presents the trapezoidal opening dimensions designed during the transition from the existing horseshoe section to the trapezoidal section for the base roads of the Ömerler underground mine. As seen in Figure 7, the gallery width was determined as 6000 mm, gallery height as 4000 mm, and trapezoidal section upper width as 5000 mm to expand the useful cross-sectional area of the gallery opening. In this case, the gallery section is calculated as 22 m². The opening dimensions considered in the empirical and numerical analysis studies for the trapezoidal section are presented as shown in Figure 7.

Table 3. Air requirements according to air velocity limits for the Ömerler coal mine [22]

| Location | Gallery Section (m ²) | Min. Air Velocity (m/s) | Req. Air Volume (m ³ /min) |
|---------------------|-----------------------------------|-------------------------|---------------------------------------|
| A1 Headgate | 16.00 | 1.0 | 870 |
| A1 Tailgate | 13.75 | 0.5 | 480 |
| A2 Coal Face | 14.50 | 0.5 | 413 |
| A6 Headgate | 13.80 | 0.5 | 414 |
| A6 Tailgate | 13.80 | 0.5 | 414 |
| Trapezoidal Section | 22.00 | 0.5 | 660 |

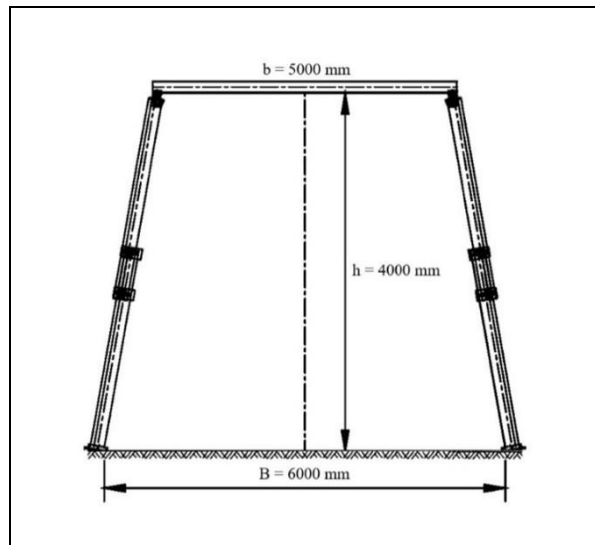


Figure 7. Dimensioning of the trapezoidal gallery section designed for numerical modeling studies

4. NUMERICAL MODELING STUDIES

4.1. Modeling Procedure

The three-dimensional numerical model of the A6 longwall panel of the Ömerler underground coal mine, where the steel set support system is applied to the main roadways and gateroads of the panels, has been created using FLAC 3D software. Two different scenarios were considered in the analysis of the models. The first scenario involves the opening of the gateroads and the implementation of support system in the A6 longwall panel's tunnel position. The second scenario involves the modeling of the coal production position, including the opening of the face, placement of face support units (self-advancing hydraulic roof support units), advancement of the face, and caving coal from the back of the face. For both positions in the created models, stress and deformation variations were examined for both trapezoidal and horseshoe sections due to the load imposed by the gateroad support units.

The coal seam in the region where the A6 longwall panel is located is approximately 161 m deep from the surface. The underlying shale, which is the base rock unit beneath the coal seam with a thickness of about 11 m, is defined in the model geometry as 39 m. The model geometry is defined as 200 m in the z-direction. The limestone unit, defined as tuffstone immediately above the coal seam with a thickness of about 140 m, is considered based on drilling logs obtained from the mine. The marl formation, consisting of limestone shale interbedded with sandstone siltstone bands, and the limestone shale roof, which together make up a large part of the 140 m layers above the coal seam, are defined in the model as the same unit due to similar mass and material properties. No separate boundary is defined for the 6 m dolerite rock unit, which constitutes approximately 4.2% of the 140 m roof unit. The 10 m topsoil fill material above the layers in the coal roof is also defined in the models.

The actual length of the A6 longwall panel is approximately 450 m. In the model, the geometry

representing the length of the panel is defined in the +y direction as 500 m. In the initial stage of modeling, which involves the opening of galleries and the implementation of support units, the gateroads were driven for 500 m. The face of the panel is defined at the 450th m in the +y direction in the model geometry, and the remaining 50 m behind it are designated as the compressed caved zone to be defined after the stages of face excavation and supporting, for the determination of the effects of the compressed caved zone and the dynamic caved zone resulting from the advancement of the face.

The other regions of the model geometry are divided into 5m and 10 m grids according to the sensitivity of the regions where stress and deformation are to be examined. The created model, in its final form, includes a total of 361,665 zones and 376,320 grid points. The model geometry created in the FLAC 3D program for the A6 longwall panel, with detailed information provided above, is generally illustrated in Figure 8.

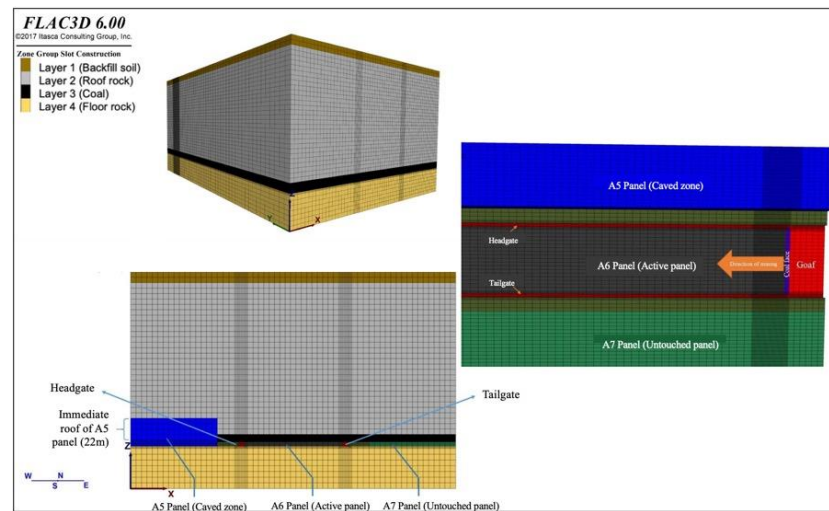


Figure 8. The geometry and details of the model created in FLAC 3D

The boundary conditions in a numerical model consist of the values of field variables (e.g., stress and displacement) that are prescribed at the boundary of the numerical grid. Boundaries are of two categories: real and artificial. Real boundaries exist in the physical object being modeled (e.g., a tunnel surface or the ground surface). Artificial boundaries do not exist in reality, but they must be introduced to enclose the chosen number of zones.

While determining the boundary conditions of the Ömerler underground coal mine model, roller boundaries are placed on the left, right, front, and rear boundaries of the grid. The bottom of the grid is fixed. The results obtained from the primary stress analyses carried out in the in-situ were defined in the model and $K_0 = 0.473$ (σ_h / σ_v) was assigned as the initial condition and gravity effect was also defined in the model.

In the model which was created by using FLAC 3D program of Ömerler underground quarry A6 longwall panel, properties of gob materials were defined and some equations were used in literature. The mechanical behavior of the gob is defined by the double-yield model in which the gob is simulated in FLAC 3D. Pappas and Mark [23] examined the behavior of longwall gob material by laboratory tests and stated that the equation presented by Salamon [24] in the gob model (1990) gave the closest results to laboratory tests. In the Salamon gob model [24], the following equation is presented (Equation 1).

$$\sigma = \frac{E_0 \varepsilon}{1 - \varepsilon / \varepsilon_m} \quad (1)$$

In Equation 1, σ ; the uniaxial stress (MPa) over the material ε ; unit deformation of the material under stresses; E_0 ; represents the initial tangent module (MPa); ε_m represents the maximum unit deformation

that can occur in the compacted rock material.

In the modeling studies, the equation given above were used to determine the mechanical behavior of the gob. Depending on the face advancement, the A6 panel is assigned a double-yield constitutive model after every 1m advance to the 1m section behind the coal face. Thus, in the model, in the early stages of face advancement, the gob region would represent a region that was broken and collapsed, unable to withstand the pressure from the roof. In this region, the gob will squeeze slowly, leading to an increase roof stress.

In the A6 longwall panel model, the resulting equation of the volumetric unit deformation behavior, deformation change values and FLAC 3D program output are determined in Table 5 and Equation 2.

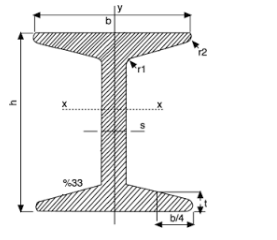
$$\sigma = \frac{29.2\varepsilon}{1-6.25\varepsilon} \tag{2}$$

Table 5. Cap pressure for the double-yield model

| Strain (m/m) | Stress (MPa) | Strain (m/m) | Stress (MPa) |
|--------------|--------------|--------------|--------------|
| 0.00 | 0 | 0.08 | 4.67 |
| 0.01 | 0.31 | 0.09 | 6.01 |
| 0.02 | 0.67 | 0.10 | 7.79 |
| 0.03 | 1.08 | 0.11 | 10.28 |
| 0.04 | 1.56 | 0.12 | 14.02 |
| 0.05 | 2.12 | 0.13 | 20.25 |
| 0.06 | 2.80 | 0.14 | 32.70 |
| 0.07 | 3.63 | 0.15 | 70.08 |

In the modeling studies, when modeling the steel set for gateroads support, a beam structural element was used. In the models, the support element input parameters used the properties of the GI profile used in the Ömerler underground mine (Table 6).

Table 6. The model's input parameters for steel set support

| | | |
|---------------------------------|---|---|
| Profile type | GI 140 |  |
| Section weight | 41.6 kg/m | |
| Dimensions | h=140 mm b=110 mm | |
| Section area | 0.0154 m ² | |
| I _x - I _y | 1586 cm ⁴ 315cm ⁴ | |
| Density | 2701.3 kg/m ³ | |

4.2. Identifying Monitoring Points in the Model

Two separate models have been prepared for three-dimensional analyses of gateroads opened in horseshoe and trapezoidal sections. In both prepared models, varying stress-deformation values were obtained for both trapezoidal and horseshoe-section gateroads at the tunnel position where the gateroads are opened (Stage-1) and at the face advancement positions where coal production is carried out (Stage-2). For monitoring the stresses and deformations generated in the model, a total of 120 monitoring points has been set up. In the evaluation of numerical analysis results, two station points located above the headgate adjacent to panels A5 and A6 have been considered. These station points are U9 located at 300 m and U3 positioned at 429 m along the material gallery (Fig. 9).

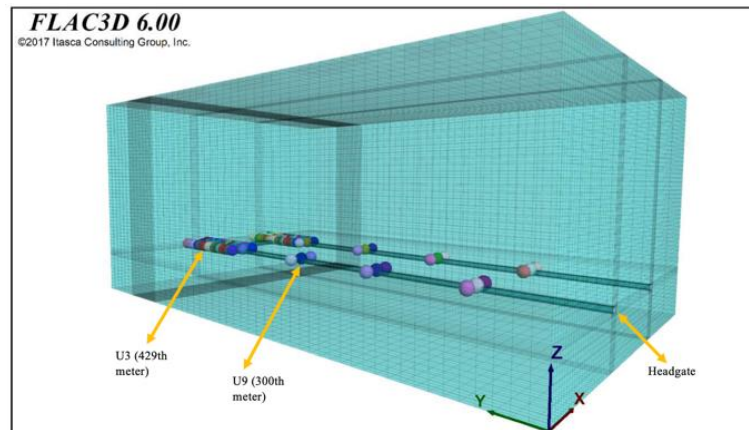


Figure 9. Location of the monitoring points on the numerical models

4.3. Assumptions and Constraints in the Model

During the modeling process, certain assumptions and constraints were considered. These are as follows:

- i. In the model studies, σ_1 is assumed to be vertical (in the $-z$ direction), and σ_2 and σ_3 are assumed to be horizontal (in the x and y directions).
- ii. The length of the A6 longwall panel, which is actually between 400 m- 450 m, was taken as 500 m in the y -direction in the model.
- iii. Material properties related to subsidence were determined using some equations available in the literature.
- iv. For defining the support units in the model, the self-advancing hydraulic roof support units were represented with shell structural elements, and the steel set support system with beam structural elements.
- v. The dip angle of the coal seam where the A6 longwall panel is located was assumed to be 0° in the model.
- vi. The groundwater was neglected in the underground water modeling studies

5. RESULT AND DISCUSSION

The gateroads of the TKI-GLI Ömerler underground mine A6 longwall panel were numerically modeled separately in horseshoe and trapezoidal sections. The results obtained for both gallery sections, contingent upon the gateroad excavation (Stage-1) and the excavation of a total of 18 m of coal of 1 m inside the coal face and the removal of the back coal (Stage-2) are presented separately below.

5.1. Numerical Analysis Results for the Horseshoe Cross Section

Throughout the process from the beginning of the excavation in the A6 gateroad with a horseshoe section until the completion of all excavation and support operations in the gateroad (Stage-1), the vertical displacement and secondary stress values at monitoring point U9, positioned at the 300th meter of the upper gateroad as schematically shown in Figure 9, were determined using FLAC 3D.

The model outputs for this condition are presented in Figure 10. Additionally, the vertical displacement and secondary stress values observed in the model outputs are presented in Table 6.

The vertical displacement and secondary stress values at monitoring point U3, located at the 429th meter of the upper gateroad and shown schematically in Figure 9, were determined using FLAC 3D for Stage-2 (Figure 11 and Table 7).

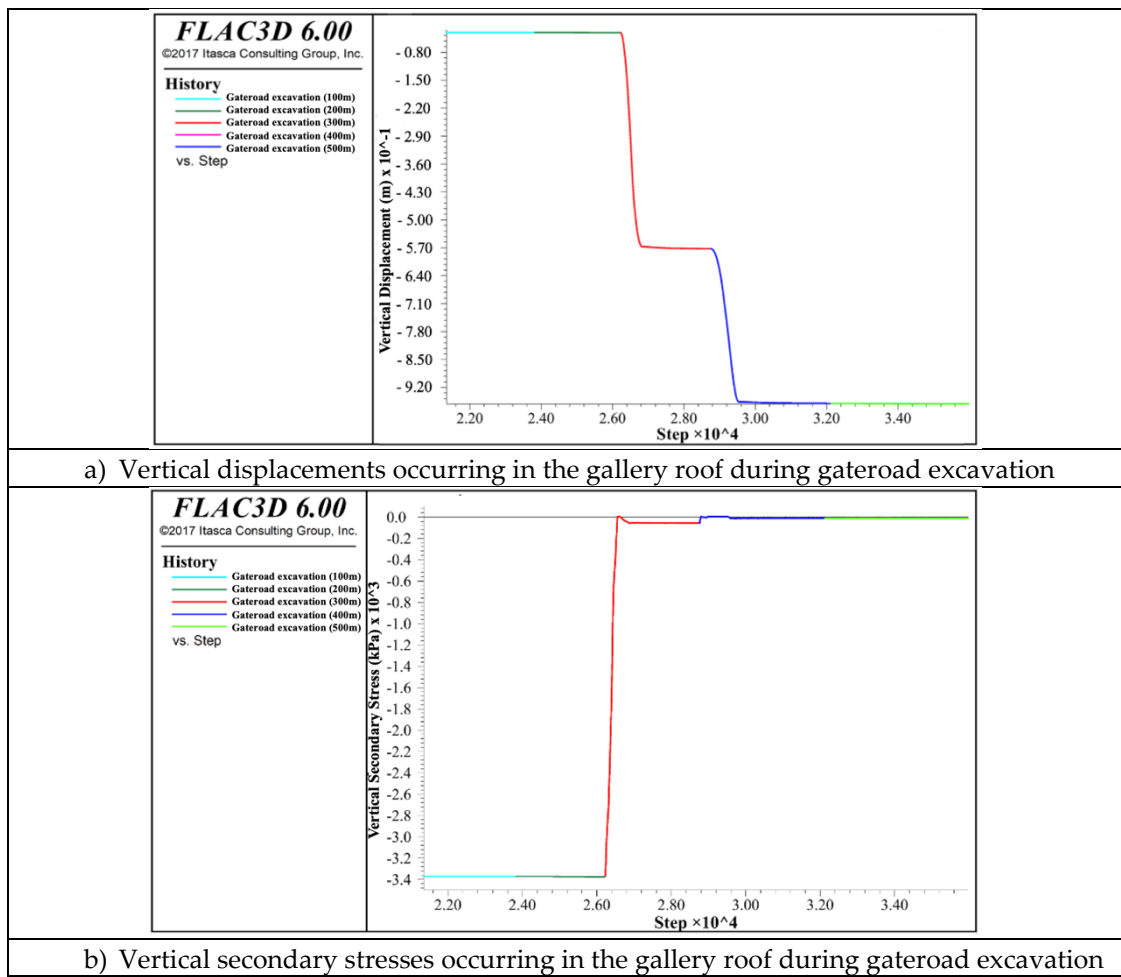


Figure 10. Vertical displacements and vertical secondary stresses for the horseshoe cross-section excavation model (U9)

Table 6. Vertical displacements and vertical secondary stress values of U9 for the horseshoe cross-section

| Gallery Excavation | Monitoring Point U9 | Monitoring Point U9 |
|--------------------|---------------------|---------------------|
| L (m) | U (mm) | P (kPa) |
| 0 | -6.5* | -3370.00* |
| 50 | -6.5 | -3367.50 |
| 100 | -6.5 | -3365.00 |
| 150 | -6.5 | -3362.50 |
| 200 | -6.5 | -3360.00 |
| 250 | -30 | -1600.00 |
| 300** | -57 | -40.00 |
| 350 | -76.6 | -30.00 |
| 400 | -96.2 | -20.00 |
| 450 | -96.2 | -15.00 |
| 500 | -96.2 | -10.00 |

* The amount of vertical displacement and secondary stress resulting from initial conditions, in monitoring point U9.

** U9 monitoring point is located at the 300th meter of excavation.

As seen in Table 6 and Figure 10, it is observed that the vertical displacement and secondary stress values remain very low up to the first 200 m as the excavation face approaches the U9 monitoring point

located at the 300th meter of the gateroad. In this situation, with still 100 m remaining to reach the U9 monitoring point, the values remain close to the initial primary values in the field. However, as the excavation face approaches the U9 monitoring point at the 300th meter, vertical displacements and secondary stresses begin to change rapidly, reaching values of $U=57$ mm and $P=-40$ kPa when the excavation face reaches the U9 monitoring point (Table 6 and Figure 10).

The numerical outputs of FLAC 3D, illustrating the vertical displacement and secondary stress values at point U3 during the progress of the gateroad excavation up to the 18th meter (Stage-2) from the start of excavation in the A6 longwall panel are presented in Figure 11. Additionally, the vertical displacement and secondary stress values observed in the model outputs are provided in Table 7.

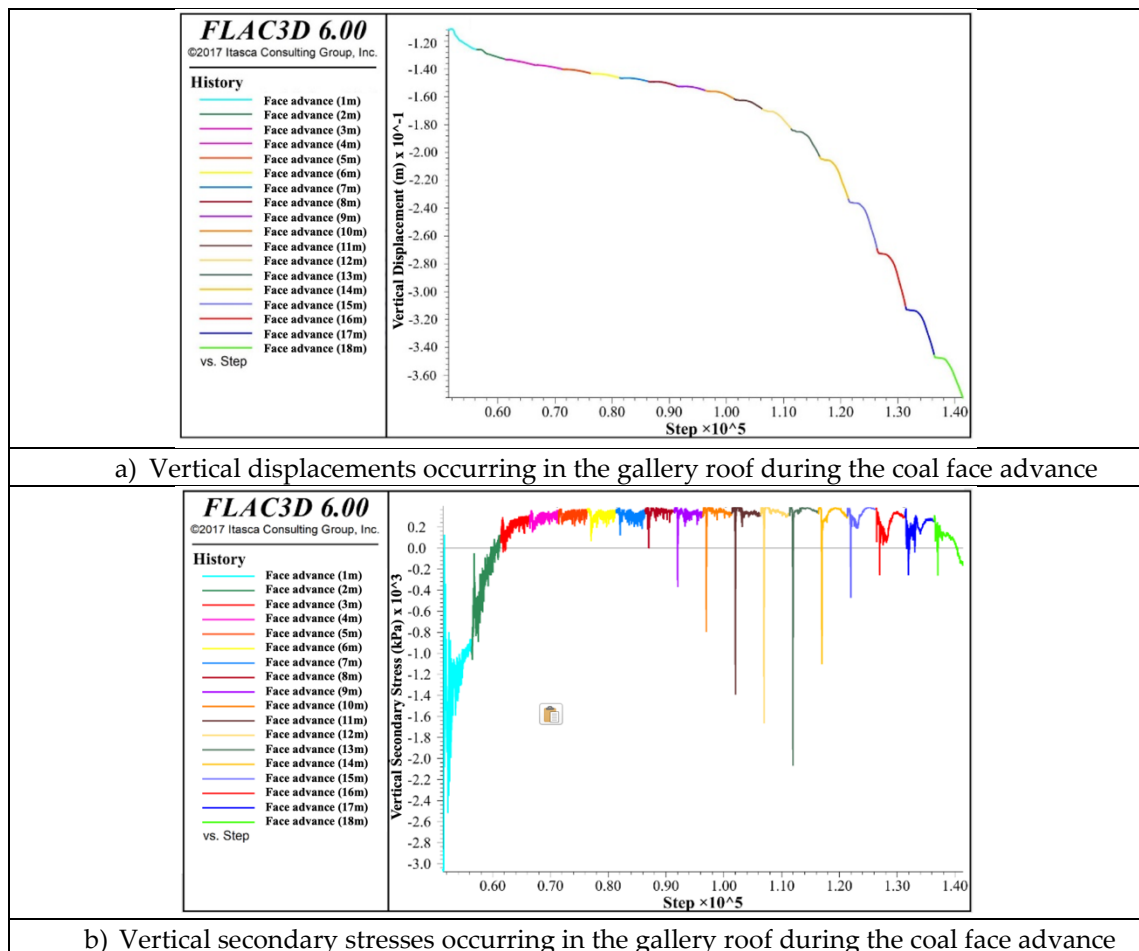


Figure 11. Vertical displacements and vertical secondary stresses for the horseshoe cross-section excavation model (U3)

As seen in Table 7 and Figure 11, the longwall advancement in the model was carried out in one-meter increments. The monitored point U3 is located at the 429th m of the gateroad. At the initial moment, this point is 18 m behind the coal face. As excavation activities progress in the longwall, displacements and stresses at the U3 monitoring point start to change. While displacements are relatively small in the first 10 m, they rapidly increase in the last 8 (Figure 11). When the longwall face advances 18 m and reaches the U3 monitoring point, the total displacement is $U=376$ mm. Stress changes initially exhibit tensile stresses and later evolve into compressive stresses. When the excavation face reaches the U3 monitoring point, the stress value in the gallery roof is $P=-1.8$ kPa (Table 7 and Figure 11).

Table 7. Vertical displacements and vertical secondary stress values of U3 for the horseshoe cross-section

| Longwall Coal Face Advancement | Monitoring Point U3 | Monitoring Point U3 |
|--------------------------------|---------------------|---------------------|
| L (m) | U (mm) | P (kPa) |
| 0 | -112.000 | -30.800 |
| 1 | -126.000 | 8.800 |
| 2 | -132.000 | 2.800 |
| 3 | -138.000 | 1.400 |
| 4 | -140.000 | 0.800 |
| 5 | -143.000 | 0.800 |
| 6 | -145.000 | 0.800 |
| 7 | -148.000 | 0.800 |
| 8 | -152.000 | 0.700 |
| 9 | -156.000 | 0.700 |
| 10 | -162.000 | 0.700 |
| 11 | -168.000 | 0.700 |
| 12 | -184.000 | 0.700 |
| 13 | -204.000 | 0.600 |
| 14 | -238.000 | 1.200 |
| 15 | -262.000 | 0.400 |
| 16 | -312.000 | 1.200 |
| 17 | -348.000 | 1.600 |
| 18* | -376.000 | -1.800 |

* U3 monitoring point is located at the 429th meter of excavation.

5.2. Numerical Analysis Results for the Trapezoidal Cross Section

The gateroad with a trapezoidal cross-section for the TKI-GLI Ömerler underground coal mine A6 panel has been modeled. The vertical displacement and secondary stress values resulting from the gateroad excavation at the monitoring point U9, as shown in Figure 9, were determined using FLAC 3D for Stage-1. The FLAC 3D outputs depicting the vertical displacement and secondary stress values at the U9 monitoring point throughout the entire process, from the moment when no excavation activities have yet started in the gateroad to the completion of all excavation and support operations in the gateroad, are presented in Figure 12. The vertical displacement and secondary stress values seen in the model outputs in Figure 12 are provided in Table 8.

As seen in Table 8 and Figure 12, it is observed that, in the model, the vertical displacement and vertical secondary stress values remain very low for the first 200 meters as the excavation face approaches the monitoring point U9, located at the 300th meter of the gateroad. In this situation, where there is still 100 meters to U9 monitoring point, the values can be stated to be close to the initial primary values in the field. However, as the excavation face approaches the U9 monitoring point at the 300th meter, vertical displacements and secondary stresses rapidly increase, reaching U=161.1 mm and P=-53.38 kPa when the excavation face reaches the U9 monitoring point (Table 8 and Figure 12).

After the excavation face passes the U9 (300th meter) monitoring point in the gateroad, the vertical displacement continues to rapidly change up to 400 meters. When the gateroad excavation face reaches from 400 meters to 500 meters, it is understood that the vertical displacement values at the U9 point in the remaining part of the gateroad almost remain constant, reaching U=271.6 mm (Table 8 and Figure 12). Similarly, after the gateroad excavation face passes the U9 (300th meter) monitoring point, the vertical stress values continue to change very little up to 500 meters. When the gateroad excavation face reaches 500 meters, it is observed that the vertical stress values at the U9 point in the remaining part of the gateroad almost remain constant, reaching P=-8.93 kPa.

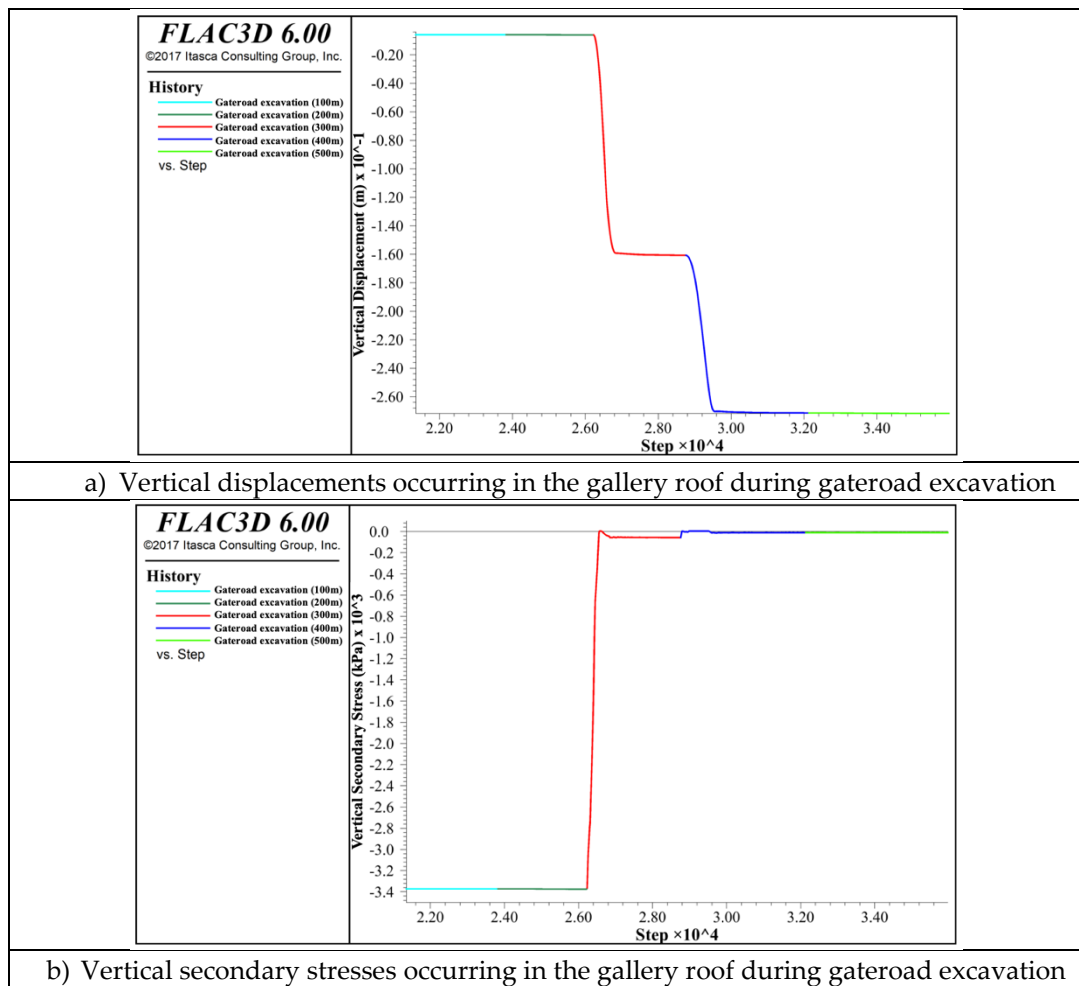


Figure 12. Vertical displacements and vertical secondary stresses for the trapezoidal cross-section excavation model(U9)

Table 8. Vertical displacements and vertical secondary stress values of U9 for the trapezoidal cross-section.

| Gallery Excavation | Monitoring Point U9 | Monitoring Point U9 |
|--------------------|---------------------|---------------------|
| L (m) | U (mm) | P (kPa) |
| 0 | -5.6* | -3371.26* |
| 50 | -5.7 | -3371.68 |
| 100 | -5.9 | -3371.96 |
| 150 | -6 | -3373.66 |
| 200 | -6.1 | -3375.08 |
| 250 | -84.4 | -1574.55 |
| 300** | -161.1 | -53.3806 |
| 350 | -216.9 | -8.93721 |
| 400 | -270.85 | -8.93725 |
| 450 | -271.4 | -8.9275 |
| 500 | -271.6 | -8.9275 |

* The amount of vertical displacement and secondary stress resulting from initial conditions, in monitoring point U9.

** U9 monitoring point is located at the 300th meter of excavation

The vertical displacement and secondary stress values at the U3 monitoring point, as shown schematically in Figure 9 and located at the 429th meter of the upper gateroad, were determined by FLAC

3D. The FLAC 3D outputs depicting the vertical displacement and secondary stress values at the U3 point during the process of gateroad excavation and the advancement of the 18-meter coal cutting within the longwall face in Stage-2, starting from the moment the preparatory activities were completed, are presented in Figure 13. The vertical displacement and secondary stress values observed in the model outputs are provided in Table 9.

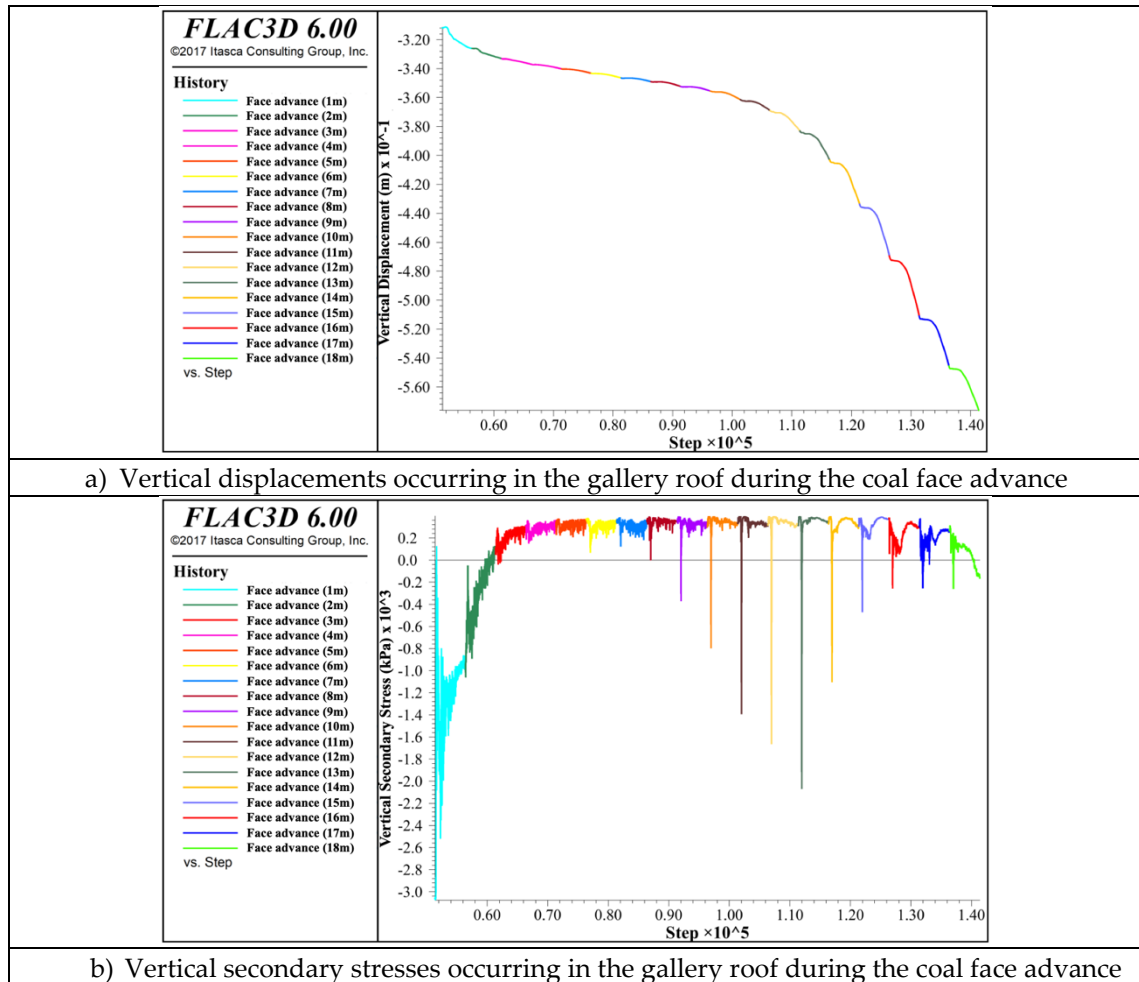


Figure 13. Vertical displacements and vertical secondary stresses for the trapezoidal cross-section excavation model (U3)

As seen in Table 9 and Figure 13, the longwall advancement in the model was carried out in one-meter increments. The monitored point U3 is located at the 429th m of the gateroad. At the initial moment, this point is 18 m behind the coal face. As excavation activities progress in the longwall, displacements and stresses at the U3 monitoring point start to change. While displacements are relatively small in the first 10 m, they rapidly increase in the last 8 (Figure 13). When the longwall face advances 18 m and reaches the U3 monitoring point, the total displacement is $U=575.77$ mm. Stress changes initially exhibit tensile stresses and later evolve into compressive stresses. When the excavation face reaches the U3 monitoring point, the stress value in the gallery roof is $P=-1.59$ kPa (Table 9 and Figure 13).

In the models prepared for the excavation of the gateroads of A6 panel, considering both horseshoe and trapezoidal cross-sections, it is assumed that Stage-1 precedes Stage-2, as indicated by their names. For Stage-1 in the model, the U9 monitoring point (300th m) has been tracked from the initiation of headgate excavation (0th m) until the completion of the gallery (500th m). Subsequently, for Stage-2, involving the top coal caving excavation, the U3 monitoring point is positioned just 18 meters ahead of the coal face (429th m). The process of approaching the coal face with 1-meter advancements and the time

until the caving is observed. Figures 14 and 15 were constructed using data from monitoring points U3 and U9 on the headgates.

Table 9. Vertical displacements and vertical secondary stress values of U3 for the trapezoidal cross-section

| Longwall Coal Face Advancement | Monitoring Point U3 | Monitoring Point U3 |
|--------------------------------|---------------------|---------------------|
| L (m) | U (mm) | P (kPa) |
| 0 | -311.345 | -30.440 |
| 1 | -325.976 | -8.9457 |
| 2 | -333.113 | 1.2661 |
| 3 | -337.038 | 2.9086 |
| 4 | -340.25 | 3.2656 |
| 5 | -343.461 | 3.6941 |
| 6 | -346.316 | 3.5513 |
| 7 | -348.814 | 3.337 |
| 8 | -352.026 | 3.348 |
| 9 | -355.237 | 3.194 |
| 10 | -361.304 | 3.265 |
| 11 | -368.441 | 3.265 |
| 12 | -382.714 | 3.194 |
| 13 | -402.698 | 3.551 |
| 14 | -433.03 | 2.980 |
| 15 | -468.715 | 3.690 |
| 16 | -510.466 | 2.980 |
| 17 | -544.723 | 2.694 |
| 18 | -575.769 | -1.590 |

* U3 monitoring point is located at the 429th meter of excavation.

5.3. Comparison of Results obtained from Numerical Analysis for both Gallery Cross Sections

The graphs presented in Figures 14 and 15 analyze all processes covering Stage-1 and Stage-2 in three sections. The first section covers Stage-1 progress (excavation advancement stage: 0-10), the second section represents the initial 50 meters of excavation for the first coal caving on the panel (excavation advancement stage: 10-11), and the third section indicates activities during Stage-2 (excavation advancement stage: 11-29). These processes are sequentially defined independently of time.

In the first part of the prepared graphs, representing Stage-1, when the gallery excavation reached the 200th m, displacements and changes in original field stresses at the yet unexcavated U3 point (300th m) are observed in Figure 14 and Figure 15. It is evident that the change of displacements is significantly higher when the headgate is excavated in a trapezoidal cross-section compared to a horseshoe cross-section. Displacement values are 161.1 mm in the trapezoidal cross-section and 57 mm in the horseshoe cross-section. Similarly, the change in secondary stresses is -53.38 kPa for the trapezoidal section and -40 kPa for the horseshoe section. It is observed that less displacement occurs in the horseshoe cross-section for Stage-1, requiring less reinforcement for the excavation (excavation advancement stage: 0-10).

For the second part of the graphs, it is assumed that the first expected collapse occurred behind the panel, and the coal face on the backside of the collapse relaxed (excavation advancement stages: 10-11).

In the third part of the prepared graphs, representing Stage-2, it is observed that displacements on the gallery ceiling rapidly increase after the coal face advance total of 10 m at 1-m intervals (excavation advancement stage: 21). This increase is much greater in the trapezoidal cross-section. Displacement values are 575.77 mm in the trapezoidal section and 376 mm in the horseshoe section. Similarly, the change

in secondary stresses is -1.59 kPa for the trapezoidal cross-section and -1.8 kPa for the horseshoe cross-section (excavation advancement stage: 11-29).

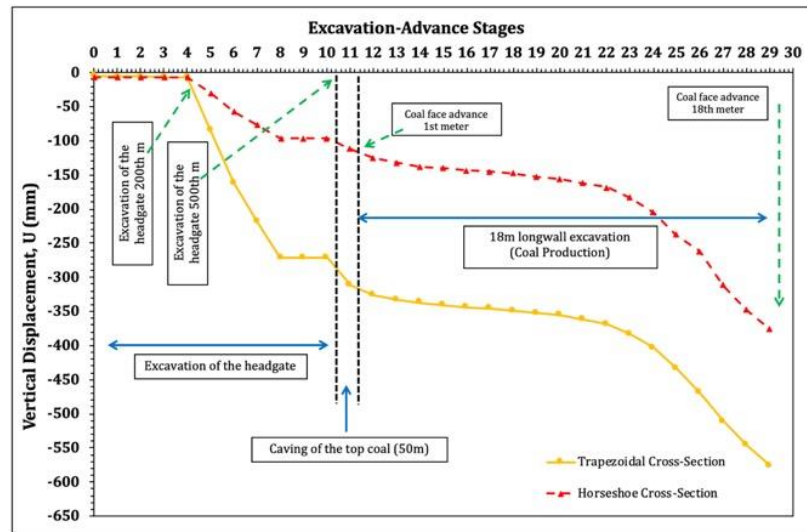


Figure 14. Vertical displacement changes in trapezoidal and horseshoe gallery cross-sections for all steps of Stage-1 and Stage-2 scenarios

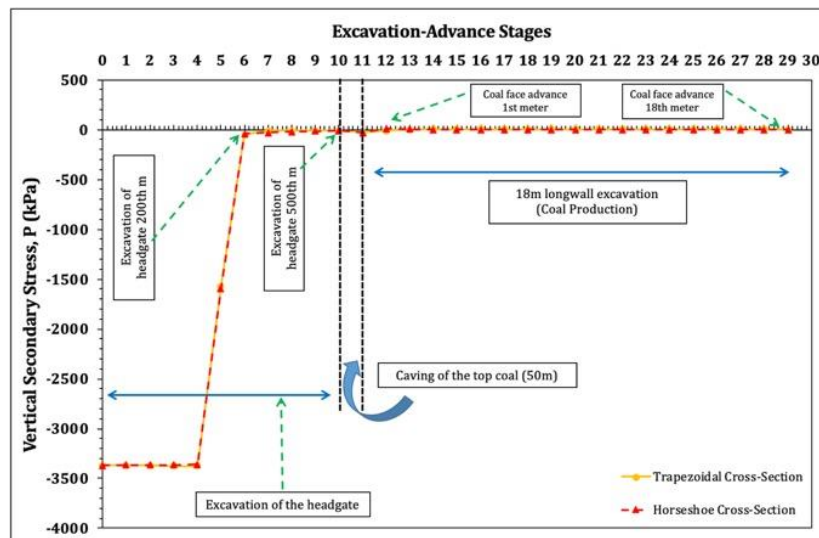


Figure 15. Vertical secondary stress changes in trapezoidal and horseshoe gallery cross-sections for all steps of Stage-1 and Stage-2 scenarios

6. CONCLUSIONS

The numerical modeling and analysis of gallery cross-sectional variation in the Ömerler underground mine, operated by the TKI-GLI, provided valuable insights into the stress-strain variations resulting from gallery cross-section changes in a LTCC panel. The study focused on the A6 panel and utilized the FLAC3D for numerical simulations. In the study, extensive field and laboratory rock mechanics studies were conducted to establish a comprehensive database. Rock mass and material properties were determined through drilling, block extraction, and various rock mechanics tests. Numerical simulations were performed using FLAC3D to model the A6 panel's gallery cross-sectional changes. Two scenarios were considered: Stage-1 involved gateroad excavation, and Stage-2 focused on coal production. Key findings and conclusions from the study include:

- i. Gallery cross-sectional variation significantly influences stress distribution in the rock mass.
- ii. Trapezoidal cross-sections showed higher vertical displacements and secondary stresses compared to horseshoe cross-sections.
- iii. The change in displacements and stresses was more pronounced in trapezoidal sections during both gateroad excavation and coal production stages.
- iv. Trapezoidal sections, while providing increased useful cross-sectional area, may lead to higher displacements and stresses.
- v. The study highlights the need for careful consideration in designing gallery cross-sections to minimize stress-induced risks.
- vi. Continuous monitoring of stress-strain variations during mining operations can inform real-time adjustments to ensure worker safety.
- vii. The study contributes to the understanding of stress-strain variations in LTCC mining and provides a basis for improving safety measures and operational efficiency.

In conclusion, the numerical modeling of stress-strain variations resulting from gallery cross-section changes in the Ömerler underground mine contributes essential insights to the field of mining engineering. It emphasizes the delicate balance between achieving operational efficiency and ensuring the safety of mining operations, shedding light on the complex dynamics of underground coal mining, particularly in the context of LTCC mining methods. In addition, it would be appropriate to compare the rock bolts design results obtained from using numerical methods for two different cross sections.

Declaration of Ethical Standards

The authors declare that the study complies with all applicable laws and regulations and meets ethical standards.

Declaration of Competing Interest

The authors declare that they have no known competing financial interests or personal relationships that could have appeared to influence the work reported in this paper.

Funding / Acknowledgements

This work was supported by the TUBITAK (The Scientific and Technological Research Council of Turkey) with a 1001 project (Project No: 116M698). The authors thanks to Turkish Coal Enterprises (TKI) and West Lignite Enterprise (GLI) staff for their help in field studies .

Data Availability

Data will be made available on request.

REFERENCES

- [1] G. Li, Z. Hu, P. Li, D. Yuan, Z. Feng, W. Wang and Y. Fu, "Innovation for sustainable mining: Integrated planning of underground coal mining and mine reclamation," *Journal of Cleaner Production*, 351, 131522, 2022.
- [2] Z. Hu, G. Li, J. Xia, Z. Feng, J. Han, Z. Chen, W. Wang and G. Li, "Coupling of underground coal mining and mine reclamation for farmland protection and sustainable mining," *Resources Policy*, 84, 103756, 2023.
- [3] International Energy Agency (IEA), *World Energy Outlook*. (2022). Accessed: July, 19, 2023. [Online]. Available: <https://www.iea.org/reports/world-energy-outlook-2022>.
- [4] A. Çelik and Y. Özçelik, "Investigation of the effect of caving height on the efficiency of the longwall top coal caving production method applied in inclined and thick coal seams by physical

- modeling," *International Journal of Rock Mechanics and Mining Sciences*, 162, 105304, 2023.
- [5] M. Shabanimashcool, and C. C. Li, "Numerical modelling of longwall mining and stability analysis of the gates in a coal mine," *International Journal of Rock Mechanics and Mining Sciences*, 51, 24-34, 2012.
- [6] M. Mesutoğlu, and İ. Özkan, "Büyük Ölçekli Kömür Arınında Gerçekleştirilen Schmidt Sertlik İndeksi ve Nokta Yükleme Dayanımı Deney Sonuçlarının Değerlendirilmesi," *Konya Mühendislik Bilimleri Dergisi*, v.7, n.4, pp. 681-695, 2019.
- [7] L. Zhou, X. Li, Y. Peng, B. Xia, and B. Fang, "Material point method with a strain-softening model to simulate roof strata movement induced by progressive longwall mining," *International Journal of Rock Mechanics and Mining Sciences*, 170, 105508, 2023.
- [8] N.E. Yaşitlı, and B. Unver, "3D numerical modeling of longwall mining with top-coal caving," *International Journal of Rock Mechanics and Mining Sciences*, v.42, i.2, pp. 219-235, 2005.
- [9] F. Şimşir, and M. K. Özfirat, "Determination of the most effective longwall equipment combination in longwall top coal caving (LTCC) method by simulation modelling," *International Journal of Rock Mechanics and Mining Sciences*, v.45, pp. 1015-1023, 2008.
- [10] T. D. Le, and J. Oh, "Longwall face stability analysis from a discontinuum-Discrete Fracture Network modelling," *Tunnelling and Underground Space Technology*, 124, 104480, 2022.
- [11] H. Wang, J. Wang, D. Elmo, M. He, Z. Ma, and C. Gao, "Ground response mechanism of entries and control methods induced by hard roof in longwall top coal caving panel," *Engineering Failure Analysis*, 144, 106940, 2023.
- [12] A. Çelik and Y. Özçelik, "Investigation of the efficiency of longwall top coal caving method applied by forming a face in horizontal thickness of the seam in steeply inclined thick coal seams by using a physical model," *International Journal of Rock Mechanics and Mining Sciences*, 148, 104917, 2021.
- [13] T. D. Le, J. Oh, B. Hebblewhite, C. Zhang, and R. Mitra, "A discontinuum modelling approach for investigation of Longwall Top Coal Caving mechanisms," *International Journal of Rock Mechanics and Mining Sciences*, 106, pp.84-95, 2018.
- [14] J. Wang, W. Wei, J. Zhang, B. Misra, and A. Li, "Numerical investigation on the caving mechanism with different standard deviations of top coal block size in LTCC," *International Journal of Mining Science and Technology*, 30, 583-591, 2020.
- [15] F. Song, A. Rodriguez-Dono, S. Olivella, Z. Zhong "Analysis and modelling of longitudinal deformation profiles of tunnels excavated in strain-softening time-dependent rock masses," *Computers and Geotechnics*, 125, 103643, 2020.
- [16] F. Song, A. Rodriguez-Dono, "Numerical solutions for tunnels excavated in strain-softening rock masses considering a combined support system," *Applied Mathematical Modelling*, 92, 905-930, 2021.
- [17] R. Çelik, "Developing of Moving Procedure for Powered Supports in Ömerler Coal Mine," Ph. D. dissertation, Osmangazi Univ. Dep. of Mining Eng., Eskişehir, 2005.
- [18] M. Mesutoğlu, "Determination of rock bolt and steel set behaviors used in control of longwall tailgate roof strata by numerical analysis," PhD dissertation, Konya Tech. Univ., Dep. of Mining Eng., Konya, 2019.
- [19] İ. Özkan, M. Geniş, Ö. Uysal and M. Mesutoğlu "New technology for roof support of coal roadways in our national underground coal mining: Design of roof bolt systems," TÜBİTAK Project No. 116M698 Final Report, Ankara, 430p. 2022.
- [20] M. Geniş, and Ö. Aydan, "Static and dynamic stability of a large underground opening," Proceedings of the second symposium on Underground excavations for Transportation (in Turkish), TMMOB, Istanbul, 2007, pp. 317-326.
- [21] Ö. Aydan, "A new stress inference method for the stress state of Earth's crust and its application," *Bulletin of Earthscience*, v.22, pp. 223-236, 2000.
- [22] A. Fişne, "Türkiye Kömür İşletmeleri Kurumu Garp Linyitleri İşletmesi Müdürlüğü Ömerler-A

- Yeraltı Kömür Ocağı Havalandırma Sisteminin Deęerlendirilmesi" Project Report. 2017.
- [23] D.M. Pappas, and C. Mark, "Behavior of simulated longwall gob material," *Report of Investigation No: 9458*, United States Department of the Interior, Bureau of Mines, 1993.
- [24] M. Salamon, "Mechanism of caving in longwall coal mining, Rock mechanics contributions and challenges" Proceedings of the 31st US symposium, 1990, pp. 161-168.